Linac Coherent Light Source soft x-ray materials science instrument optical design and monochromator commissioning

Philip Heimann,[1,2] Oleg Krupin,[2,3] William F. Schlotter,[2] Joshua Turner,[2] Jacek Krzywinski,[2] Florian Sorgenfrei,[4] Marc Messerschmidt,[2] David Bernstein,[5] Jaromir Chalupský,[6] Vera Hájková,[6] Stefan Hau-Riege,[7] Michael Holmes,[2] Libor Juha,[6] Nicholas Kelez,[2] Jan Lüning,[8] Dennis Nordlund,[9] Monica Fernandez Perea,[7,10] Andreas Scherz,[5] Regina Soufli,[7] Wilfried Wurth,[4] and Michael Rowen[2]

[1]*Advanced Light Source, Lawrence Berkeley National Laboratory, Berkeley, California 94720, USA*
[2]*Linac Coherent Light Source, SLAC National Accelerator Laboratory, Menlo Park, California 94025, USA*
[3]*European XFEL GmbH, 22761 Hamburg, Germany*
[4]*Institut für Experimentalphysik and Centre for Free-Electron Laser Science, Universität Hamburg, Luruper Chaussee 149, 22761, Hamburg, Germany*
[5]*Stanford Institute for Materials & Energy Science, SLAC National Accelerator Laboratory, Menlo Park, California 94025, USA*
[6]*Institute of Physics, Academy of Sciences of the Czech Republic, Na Slovance 2, 182 21 Prague 8, Czech Republic*
[7]*Lawrence Livermore National Laboratory, Livermore, California 94550, USA*
[8]*Laboratoire de Chimie Physique – Matière et Rayonnement, UMR 7614 CNRS, Université Pierre et Marie Curie, Paris, France*
[9]*Stanford Synchrotron Radiation Lightsource, SLAC National Accelerator Laboratory, Menlo Park, California 94025, USA*
[10]*Consejo Superior de Investigaciones Cientificas, C/ Serrano 144 28006 Madrid, Spain*

(Received 1 July 2011; accepted 15 August 2011; published online 12 September 2011)

We present the x-ray optical design of the soft x-ray materials science instrument at the Linac Coherent Light Source, consisting of a varied line-spaced grating monochromator and Kirkpatrick-Baez refocusing optics. Results from the commissioning of the monochromator are shown. A resolving power of 3000 was achieved, which is within a factor of two of the design goal. © *2011 American Institute of Physics*. [doi:10.1063/1.3633947]

I. INTRODUCTION

At the Linac Coherent Light Source (LCLS) free electron laser (FEL),[1] the soft x-ray materials science (SXR) instrument was designed to serve a user community, which investigates a wide range of scientific problems including catalysis, magnetism, correlated materials, and aqueous solutions. The majority of the research projects aims at studying phenomena on the femtosecond timescale in these materials using time-resolved x-ray spectroscopy. An x-ray free electron laser has a spectrum with a strong fundamental peak and weak harmonics.[2] In comparison to bend magnets or undulators at synchrotron radiation facilities, the bandwidth of the x-ray FEL fundamental is relatively narrow, about 0.5% for the LCLS at soft x-ray photon energies. However, many soft x-ray spectroscopy experiments require higher energy resolution, which must be provided by a monochromator. For the SXR instrument, it is also important to be able to operate in a non-monochromatic mode, providing the intrinsic FEL bandwidth at higher intensities. The monochromator and the optical system were designed to access the energy range of 500 – 2000 eV, which covers several of the important K and L absorption edges of the second and third row elements and makes possible resonantly exciting these elements. For example, the monochromator and the optical system are designed to reach the N and O K edges and first row transition metal L edges. The lower part of this energy range, below 800 eV, is outside of the original specifications of what the LCLS would deliver.

For the monochromator design, an energy resolution, $E/\Delta E$, of 5000 from 500 to 1000 eV was specified whereas the resolution requirement above 1000 eV was lower (2500 at 2000 eV). This energy resolution will allow for a selective excitation at specific x-ray absorption resonances with a reasonable temporal broadening of the LCLS x-ray pulse for pump-probe experiments. The design goal was for the monochromator to stretch the x-ray pulse by less than 100 fs. The nominal long wavelength FEL pulse duration was calculated to be 300 fs full width at half maximum (FWHM).[2]

There are post monochromator focusing optics to image the beam in the endstations. The resolution of x-ray emission spectrometers without an entrance slit is sensitive to the focus in one dimension, generally the vertical. Coherent imaging of single molecules would profit from a smaller focus in both dimensions. The experimental station focus requirement was specified at $\leq 10 \times 10$ μm, with a smaller focus of 3×3 μm tried on a best effort basis. The divergence at the focus was given an upper limit of 1 mrad as required by holographic imaging experiments.

At synchrotron radiation sources, one of the most successful types of grating monochromators is the varied-line-spacing grating monochromator (VLS). The VLS monochromator was developed by Underwood and Koch at the Advanced Light Source.[3] A spherical mirror produces a

converging beam in the vertical plane and a varied-line-spacing grating diffracts the x-rays onto an exit slit. The variable period of the grating provides additional parameters to keep the focal distance constant as a function of photon energy and to compensate for aberrations of the spherical mirror. The focal plane is erect, i.e., perpendicular to the x-ray beam direction, which is convenient for implementing a spectrometer mode, in which the spectrum is imaged onto a detector near the exit slit location. The VLS monochromator is also rather simple mechanically in that the photon energy is scanned by a single rotation of the grating and only two optical elements are required. The limited photon energy range of the SXR instrument, 500 to 2000 eV, can be achieved without difficulty by the VLS grating monochromator design.

This paper presents the x-ray optical design of the LCLS SXR instrument and the commissioning of the SXR grating monochromator. Section II describes the optical design of the SXR monochromator and Kirkpatrick-Baez mirrors. Section III contains the results of the monochromator commissioning, which was performed during May and early June, 2010. The characterization of the focus of the SXR Kirkpatrick-Baez mirrors has been separately described in Chalupsky *et al.*[4]

II. OPTICAL DESIGN

The SXR instrument represents the second grating monochromator installed at an x-ray free electron laser. The first is the plane grating monochromator beamline at FLASH, which was designed to operate mainly at lower photon energies below the carbon K-edge at ~280 eV.[5] The optical layout of the SXR Instrument is shown in Figure 1. Table I is a list of the optical elements and their parameters. Following the LCLS undulator and upstream of the SXR instrument in the LCLS front end enclosure (not shown in Figure 1), three plane mirrors[6] in the soft x-ray offset mirror system (SOMS) separate the FEL x-rays from the high energy spontaneous and bremsstrahlung radiation. In addition, the horizontally deflecting SOMS mirrors are part of a switch yard directing the x-ray beam to the different LCLS x-ray instruments. The first component of the SXR instrument is a transmission sample system, which is a location for samples in the unfocused non-monochromatic beam. Next, there is the M1 spherical mirror and the G1 and G2 plane gratings of the VLS monochromator. In monochromator mode, an exit slit selects a narrow bandwidth of the focused FEL beam. Alternatively in spectrometer mode, a detector measures the dispersed x-ray absorption spectrum. The spectrometer detector consists of a cerium-doped yttrium-aluminum-garnet (Ce:YAG) crystal, a 45° mirror, and an optical camera. The M2 plane elliptical mirror provides the horizontal focus at the endstation location while the plane elliptical M3 mirror produces a vertical image of the exit slit in the endstations. At the SXR instrument, endstations are brought by external experimental teams for a beamtime allocation and then later replaced by a different endstation. These endstations provide the environment for a particular type of experiment, for example in surface science, using focused monochromatic or non-monochromatic beam. The transmission sample system, the M1 mirror and the gratings are in the first hutch of the LCLS near experimental hall. The rest of the beamline from the exit slit and detector through the endstation location is in the second hutch.

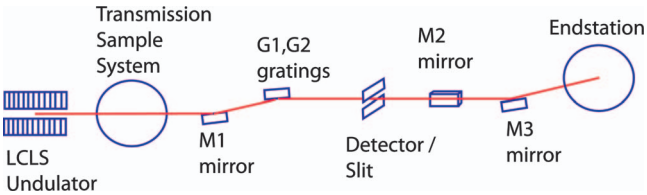

FIG. 1. (Color online) Optical layout of the SXR instrument.

The design of the optical elements follows characteristics of the LCLS SOMS mirrors in the front end enclosure.[6] The incidence angle of the mirrors is 89.20° equivalent to a grazing angle of 14 mrad. The mirror substrates are single crystal silicon, and the reflective coating is B_4C. The reflectivity of B_4C is excellent, about 90% over the whole energy range of the SXR instrument. The incidence angle and the coating materials maintain 2000 eV as the high photon energy limit. The clear apertures are set to accept a 5 σ footprint of the x-ray beam including a tolerance of 0.5 μrad rms for the LCLS beam pointing stability. The SXR instrument is based on the predicted performance of the LCLS. In particular at the LCLS, the observed divergence of the x-rays is larger than the

TABLE I. The optical elements of the SXR instrument.

	Type	Coating, blank material	Dimensions l × w × t (mm)	Radius (m)	Figure error	Roughness (nm)	Incidence angle (°)	Grating period (l/mm) order	Distance from source (m)
Transmission sample system									124
M1	Spherical mirror	B_4C, silicon	300 × 110 × 75	1049	0.3 μrad 2 nm	0.4	89.20	…	125.1
G1, G2	Plane VLS grating	B_4C, silicon	220 × 50 × 23	∞	0.3 μrad 2 nm	0.4	88.56−89.03	1/100, 1/200 −1	125.4
Detector/ Slit									132.9
M2	Bent elliptical mirror	B_4C, silicon	400 × 25 × 25	282	0.3 μrad 2 nm	0.4	89.20	…	137.4
M3	Bent elliptical mirror	B_4C, silicon	400 × 25 × 25	165	0.3 μrad 2 nm	0.4	89.20	…	137.9
Endstation									139.4

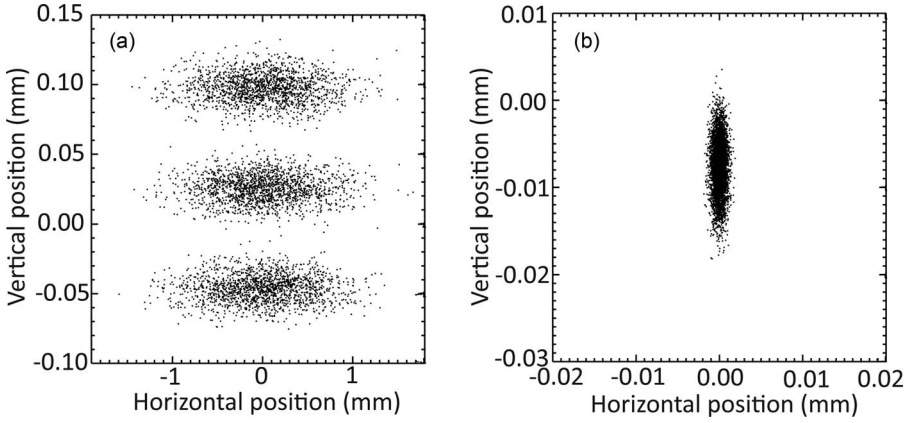

FIG. 2. (a) Photon energies 999.8, 1000, and 1000.2 eV at the exit slit. (b) The monochromatic focus at an endstation.

calculated divergence. In this section, the SXR optical design is presented in terms of the original, calculated LCLS source parameters.

The M1 mirror is polished as a sphere. On the other hand, the M2 and M3 mirrors are polished as flats and then bent into their plane elliptical shapes. The M2 and M3 mirrors need an elliptical surface in order to eliminate the coma aberration. The motorized bending of the M2 and M3 mirrors allows the focal lengths to be increased in order to enlarge the beam cross section on samples, which may suffer beam damage. In addition, the M2 and M3 bending provides flexibility for various chambers, in which the sample may be positioned at a different distance from the mirrors. The coarse grating line densities, 100 and 200 l/mm, are a consequence of the included angle 2θ being close to 180°. Both rulings are fabricated into a single grating substrate. The gratings operate in the negative first diffracted order. The choice of negative order has two benefits. The larger grazing incidence angle reduces the required length of the grating. The grating in negative order also has a magnification greater than one, which eases the needed detector spatial resolution. For the distances of the optical elements, the source position is estimated as 10 m upstream from the end of the undulator, which is an approximate LCLS source position for the soft x-ray photon energy range. More details about the B_4C coating, metrology, and calibration of the SXR mirrors and gratings can be found in Ref. 7.

Ray tracing has been performed to confirm the optical design using the XOP software.[8] Spot diagrams are displayed in Figure 2. These examples consider a photon energy of 1000 eV and the 200 l/mm grating. The LCLS FEL source was predicted to be round with a diameter of 82 μm FWHM and a divergence of 8 μrad FWHM. Compared with third generation synchrotron sources, the horizontal beam size and the divergence in both dimensions are significantly smaller. In the transmission sample system the unfocused x-ray beam is again round with a diameter of 1 mm (FWHM). The M1 mirror and VLS grating produces a vertical focus, 1.1 mm horizontal by 23 μm vertical (FWHM), at the exit slit or detector. The spot diagrams in Figure 2(a) show three different energies 999.8, 1000, and 1000.2 eV at the exit slit. The fact that these three photon energies are well resolved confirms that the resolution goal of 0.2 eV is achievable at this energy. The M2 and M3 mirrors refocus the x rays horizontally and vertically into the endstation, where the exit slit width is imaged in the vertical. In Figure 2(b), the predicted monochromatic focus in the endstations is between 1 and 2 μm horizontal by 7 μm vertical (FWHM). In the case of the non-monochromatic beam, the vertical focusing is changed because now the grating has a magnification of unity. For the non-monochromatic beam, the calculated focus in the endstations is nearly round between 1 and 2 μm in diameter (FWHM). It should be noted that this ray tracing does not include optical fabrication errors.

The tolerances for FEL x-ray optics are quite demanding and beyond, what is needed for the synchrotron radiation optics. This requirement can be simply understood by the fact that the FEL and synchrotron source dimensions are similar but for FELs, the first optic is roughly ten times further away; hence the allowable slope error is reduced by about an order of magnitude. The required tangential slope error Δ_T is given by,

$$2\,\Delta_T\, r \leq \frac{s}{2}, \tag{1}$$

where r is the source distance and s is the source dimension. Optical tolerances are included in Table I for the slope error, surface height, and roughness. The figure tolerance for the M1 mirror is the most critical to the monochromator energy resolution goal because the image created by the M1 mirror is magnified by the grating. The figure of the M2 and M3 mirrors affect the minimum focus in the endstations. The B_4C coatings place an upper limit on the roughness for spatial periods from 20 nm to 2 μm, the atomic force microscope measurement range. Substrate roughness propagates through the B_4C coating. Because the FEL x-ray beam has transverse coherence, a height specification of the optical surface is required. A Fourier optics analysis has been performed to define this requirement.

The SXR beamline optics consists of four horizontally deflecting mirrors (three SOMS mirrors and one SXR focusing mirror) and three vertically deflecting elements (two focusing elements and one grating). The Marechal criteria for well-corrected optics calls for an overall rms wavefront

distortion smaller than $\lambda/14$. The SOMS mirrors cause wavefront distortions mostly in the tangential (horizontal) direction, which is perpendicular to the dispersion direction of the grating. Therefore, the main wavefront distortions at the exit slit position come from the spherical M1 mirror and the grating. Applying the Marechal criterion and treating the errors from each optics independently, we obtain the following equation:

$$2h_{\mathrm{rms}}\theta_g\sqrt{N} \leq \frac{\lambda}{14}, \tag{2}$$

where θ_g is the grazing angle of incidence and N is the number of optical elements. We conclude that a height error h_{rms} of 2 nm should be sufficient for a diffraction limited monochromator at a photon energy of 1 keV.

For the focusing at the endstations, the Marechel criterion (Strehl ratio$<$ 0.8) calls for 1.6 nm rms height error for the horizontally deflecting optics (four optical elements) and 1.8 nm for the vertically deflecting ones (three optical elements). The quality of the wavefront in the horizontal dimension will be set mainly by the three SOMS mirrors, which had a specification of 2 nm rms height error. Therefore, the requirements of a 2 nm height error for the SXR optical elements are a reasonable choice.

The simulations were performed using a fast Fourier transform implementation of Fourier optics in a paraxial approximation.[9] The optical elements were modeled as infinitely thin phase shifters, and the problem of simulating the SXR instrument was reduced to the proper description of phase shifters and to the propagation of the wavefront in vacuum between the phase shifters.

We have used the following relationship between the phase shift $\Delta\varphi(r)$of the optical element and the optical surface profile $h(\vec{w})$:

$$\Delta\varphi(\vec{r}) = \frac{2\pi}{\lambda}\left\{n(\vec{w}) + R_0 + L - \left[\begin{array}{l}\sqrt{(R_0\cos(\alpha) - h(\vec{w}))^2 + (R_0\sin(\alpha) + w)^2} + \\ \sqrt{(L\cos(\beta_m) - h(\vec{w}))^2 + (L\sin(\beta_m) + w)^2}\end{array}\right]\right\}, \tag{3}$$

where the two-dimensional vector $\vec{r} = [x, y]$, perpendicular to the wavefront propagation direction, and the vector $\vec{w} = [w_t, w_s]$, having components parallel to the tangential and the sagittal directions respectively, are related by the equation, $[x, y] = [\cos(\beta_m)w_t, w_s]$. Here, R_0 is the mean radius of curvature of the incident wavefront, L is the mean radius of curvature of the diffracted wavefront, α is the angle of incidence with respect to the normal, β_m, $m = 0, \pm1, \pm2, \ldots$. is the diffraction angle. In the case of a mirror $m = 0$ and $\alpha = \beta_0$. For $m \neq 0$, the angle β_m is determined from the grating equation. $n(w)$ is the groove number. It can be expanded as a power series of w, $n(w) = 1/\sigma_0(w + n_2w^2 + n_3w^3 + \cdots)$, where σ_0 is the grating period at the origin. In our case, $n(w)$ was controlled up to third order expansion in w to assure the proper focusing and to minimize the third order aberration introduced by the spherical M1 mirror.

The surface errors were generated from power spectral density (PSD) functions that reflected the specifications of SOMS and as well as measurements of SOMS sample mirrors. The part of the PSD, which makes the most significant contribution to the overall rms height error, is the low spatial frequency part. The lowest spatial frequency that contributes is in order of $\theta_g/b \approx 0.014$ mm^{-1} in the tangential direction and $1/b \approx 1$ mm^{-1} in the sagittal direction, respectively. Here, b is the beam size at the optical element. The 1 mm^{-1} spatial frequency is close to the range of mid-frequency roughness which is typically $\sim$0.5 nm rms for good quality optics. Therefore, the mirrors and the grating will disturb the wavefront mainly in the tangential direction.

An example of the simulated focus of the SXR monochromator for 2 nm rms quality optics is presented in Figure 3. From the Fourier optics calculation, the width of the focus at the exit slit confirms the prediction of the ray tracing that a resolving power of 5000 is achievable. However in Figure 3, non-Gaussian tails are seen on the sides of the images of each photon energy. The predicted non-Gaussian profile of the monochromator focus could complicate the observation of a weak spectral feature near a strong one.

The grating efficiency is the most important contribution when determining the overall beamline efficiency. Efficiency calculations were performed with the GSOLVER code and are displayed in Figure 4.[10] The optical constants

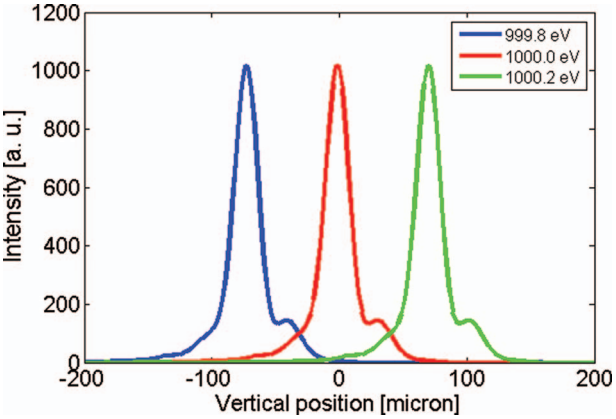

FIG. 3. (Color online) A Fourier optics simulation of the focus at the exit slit.

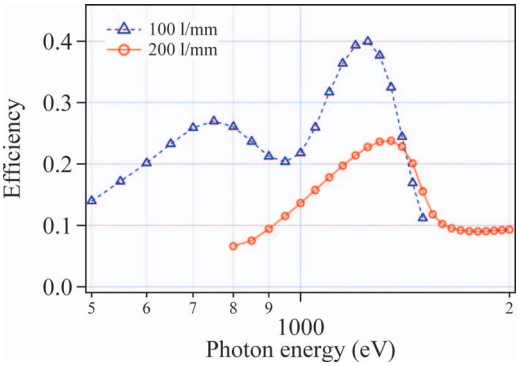

FIG. 4. (Color online) A calculation of the efficiency of the 100 and 200 l/mm gratings.

for the B_4C coating were taken from the center for x-ray optics (CXRO) website.[11] Now, experimentally determined optical constants for B_4C are available in Ref. 12. For the laminar groove profiles, the groove depths and widths were varied to maximize the efficiency at single photon energies: 800 eV for the 100 line/mm grating and 1200 eV for the 200 line/mm grating. The optimal groove depths were found to be 19 nm for the 100 line/mm and 13 nm for the 200 line/mm grating. High efficiencies between 0.07 and 0.40 were calculated. These efficiencies should be related to the low groove densities and the high reflectivity of B_4C. In Ref. 7, measured efficiencies of the SXR gratings are presented together with calculations, where the groove profiles are varied in order to obtain the best agreement with the measurements.

The average power in the LCLS FEL radiation is low, 0.2 W, because of the low repetition rate, 120 Hz. As a consequence, no water-cooling is required for the SXR x-ray optics. On the other hand, the peak power is quite high, ~5 GW, as a result of the ultrashort pulses. Optical damage from the LCLS x rays has been modeled by London *et al.*[13] The design criterion is to stay significantly below the melt fluence. Damage measurements have also been performed with x-ray FEL beams, which have confirmed that the single pulse damage threshold is comparable to the melt fluence.[14] The risk of optical damage is reduced by using small grazing angles and low Z coatings. The SXR mirrors employ essentially the same incidence angle and the same coating as the LCLS soft x-ray offset mirrors. The calculated absorbed doses are shown in Table II. For all the x-ray optics, the absorbed energy is well below melting dose of 0.62 eV/atom. For the gratings, two cases were considered: the grazing incidence illumination of the lands and grooves and the leading edges of the lands, where the x rays strike at near-normal incidence. However, estimates of both these cases gave acceptable maximum doses. For the grazing incidence optics, the photon energy corresponding to the maximum absorbed dose is in the range of 1820 to 1910 eV. The absorbed dose increases at higher photon energies because of the smaller beam divergence. Electron transport away from the optical absorption depth[13] has not been included in these calculations. This effect would further reduce the absorbed dose per atom. The optics of the SXR instrument are predicted to be undamaged by the FEL radiation.

TABLE II. Calculation of the absorbed dose for the SXR optics.

Optic	Maximum absorbed dose (eV/atom)
M1 mirror	0.050
Gratings	0.065 (grazing), 0.052 (near-normal)
M2 mirror	0.068
M3 mirror	0.076

The exit slit may be also damaged from the LCLS FEL beam, which is vertically focused at this location. Three cases must be considered: monochromatic beam, zero order beam, and non-monochromatic beam. For the monochromatic situation the dose is acceptable, 0.03 eV/atom, because the intensity is reduced by the dispersion of the different FEL wavelengths in the negative first order. The zero order can be blocked at a small distance downstream of the gratings, where the x-ray beam is not focused. The final and most difficult case is the undispersed non-monochromatic beam. Here, the dose at the exit slit, 5 eV/atom, is not acceptable. This accident condition is resolved by the machine protection system, which restricts the range of the grating angles in the non-monochromatic operational mode and requires that the exit slit be open. These damage considerations lead to the exit slit blades being made of B_4C.

Grating optics increase the x-ray pulse duration. This pulse stretching, Δt, results from the extra optical path, $m\lambda$, between groove n and groove $n+1$, where m is the order of diffraction and λ the x-ray wavelength. It can be calculated from

$$\Delta t = \frac{Nm\lambda}{c}, \tag{4}$$

where N is the number of illuminated grooves and c is the speed of light. For the 800 eV and the calculated LCLS source parameters, the estimated pulse stretching is 30 fs, which is well below the predicted LCLS pulse duration of 320 fs. Here, the calculations overestimated the operational pulse duration, which in the normal mode can be set in the range of 60 to 300 fs. In addition, LCLS has a low charge mode, in which the pulse duration is estimated to be <10 fs. For measurements with the sample in the transmission sample system or in the endstations using non-monochromatic beam, there is no optical pulse stretching. There is an aperture with the SXR monochromator, which can restrict the illumination of the grating tailoring the pulse stretching with a corresponding loss in intensity and in energy resolution.

Switching between monochromatic and non-monochromatic operation is accomplished by a translation of the grating carriage, which moves the ruled or unruled areas of the grating to the x-ray beam location.

III. COMMISSIONING OF THE SXR MONOCHROMATOR

The SXR monochromator commissioning included the x-ray alignment, the determination of the energy resolution, and the photon energy calibration. The SXR instrument had to adapt to changes in the LCLS operating parameters. The

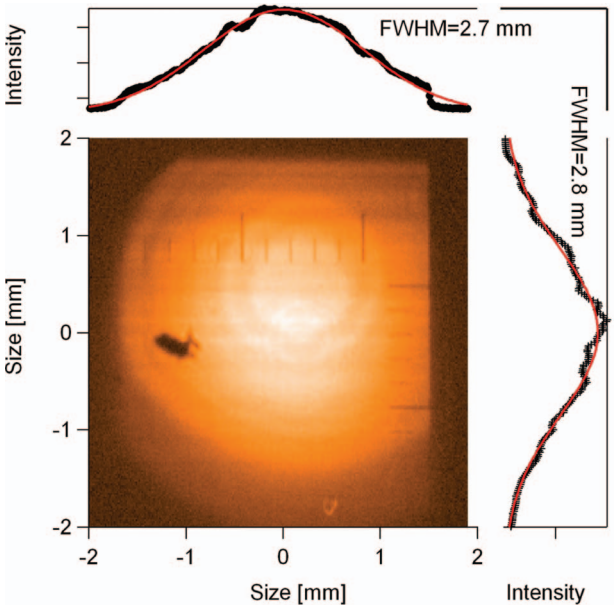

FIG. 5. (Color online) The x-ray beam profile in the transmission sample system.

observed divergence of the LCLS x-rays is a factor of two larger than the predicted divergence. In addition, the source point was moved 40 m further from the SXR instrument when 10 undulators were removed to prepare for a second harmonic after burner. To observe the x-rays coming into the SXR instrument, the beam profile was detected on a Ce:YAG crystal in the transmission sample system. The LCLS photon energy was set near the iron L edges at 714 eV. The observed beam profile displayed in Figure 5 represents a divergence of 16 μrad in the horizontal direction and 17 μrad in the vertical. This observation is in agreement with the current calculations for the LCLS nominal operating mode at this photon energy.

The M1 pitch angle was adjusted while observing the zero order focus at the spectrometer detector behind the exit slit. Figure 6 shows the zero order focus following the optimization of the M1 pitch angle. The photon energy was 1600 eV, and the gas attenuator was set to a transmission of 0.001 in order to avoid saturation effects. A Gaussian fit of the zero order focus results in a 21 μm FWHM. It should be noted that this focus includes non-Gaussian tails. The observed width of the zero order focus is in satisfactory agreement with the calculated value of 15 μm from geometric optics including the optical figure errors. The spatial resolution of the spectrometer detector may make a significant contribution to the measured zero order width, which corresponds to 5 pixels in the detector image. The zero order shows that the focusing of the M1 mirror and grating is satisfactory and implies that the energy resolution should approach the design values. The small non-Gaussian tails observed in the zero order focus are in qualitative agreement with the Fourier optics simulation shown in Figure 3. The measured focus profile could also be influenced by the thickness of the Ce:YAG crystal, 1 mm at that time.

In order to characterize the SXR monochromator resolution, neon and xenon were introduced into a gas

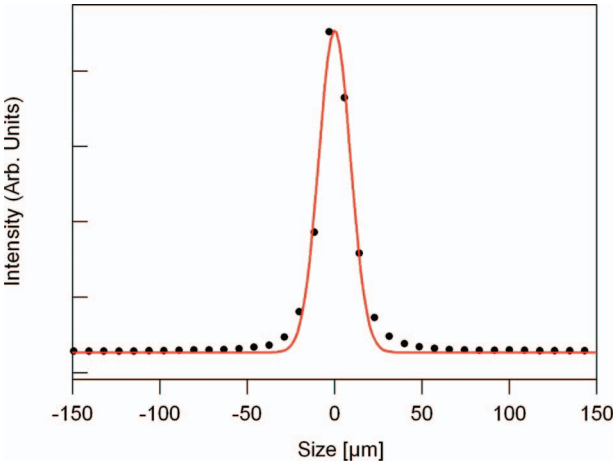

FIG. 6. (Color online) The zero order focus at the spectrometer detector.

absorption cell located upstream of the SXR monochromator. Two aluminum windows, 200 nm thick, installed in O-ring-sealed inserts in manual gate valves permit a 703 mm long region of gas to be introduced, separate from the vacuum of the rest of the beamline. With the gate valves open the instrument operates without aluminum or gas in the x-ray beam path. In this way, narrow features in the x-ray absorption spectra were observed in transmission. The LCLS x-ray bandwidth, 0.5% for soft x rays,[1] is narrow compared with a near-edge x-ray absorption spectrum. In order to provide a wider photon energy range, the LCLS was run in two modes. In the first mode, the electron beam energy is stepped every few seconds around a central energy. This modulation increases the photon energy bandwidth, but the I_0 spectrum varies in time. In a second mode, the electron bunch was given an energy chirp, which also leads to a larger x-ray bandwidth.

The neon 1*s* x-ray absorption spectrum was measured for both grating rulings. In Figure 7 the spectrum is shown for the 200 l/mm grating and in Figure 8 the spectrum with the 100 l/mm grating. A neon pressure of 100 mTorr was used to be in the linear regime. For the M1 mirror, different optimal pitch angles were found for the 200 l/mm grating first order, for the 100 l/mm grating first order, and for the zero order. This necessity to vary the M1 pitch angle will be discussed further below. I_0 spectra were measured without neon gas for normalization. The resonances were fit to Gaussian functions. The natural lifetime broadening ΔE_L of the neon 1*s*–3*p* resonance is 0.25 eV.[15] From a simple quadratic subtraction of the total resolution ΔE_T,

$$\Delta E_T = \sqrt{\Delta E_M^2 + \Delta E_L^2}, \tag{5}$$

we infer an instrumental resolution $\Delta E_M$of 1/3500 for the 200 l/mm grating and 1/2000 for the 100 l/mm grating at this photon energy.

Figure 9 shows the xenon $3d_{5/2}$ x-ray absorption spectrum measured with the 100 l/mm grating. The xenon pressure was 500 mTorr. This spectrum contains an isolated resonance $3d^{-1}{}_{5/2}$-6*p*, for which Kato *et al.*[16] report a natural linewidth of 0.42 eV. From a quadratic subtraction of the

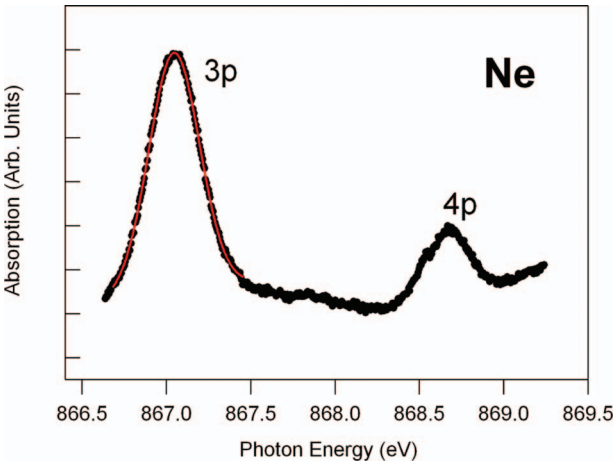

FIG. 7. (Color online) The neon 1*s* x-ray absorption spectrum taken with the 200 l/mm grating.

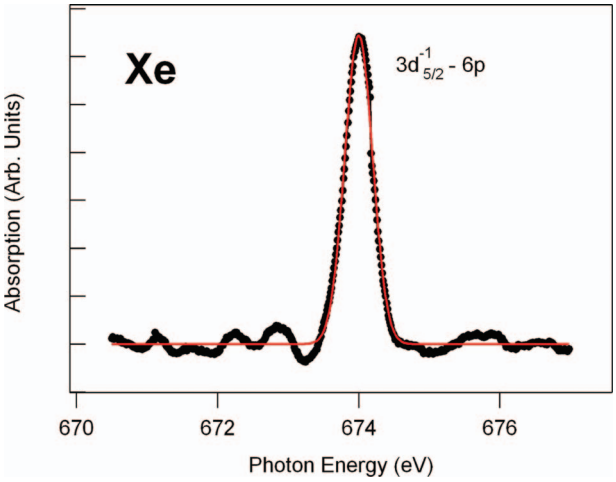

FIG. 9. (Color online) The xenon $3d_{5/2}$ x-ray absorption spectrum measured with the 100 l/mm grating.

natural linewidth, we infer an instrumental resolution of 1/3200 for the 100 l/mm grating at this photon energy.

Different M1 pitch angles are required to optimize the monochromator focusing for the zero order and for the first order of the 100 and 200 l/mm gratings. According to the VLS grating monochromator design, the M1 mirror should have one alignment for both zero and first order and for both grating rulings. The maximum M1 angle change is 0.5 mrad between zero order and first order for the 200 l/mm grating. The cause of the different M1 focus conditions is inferred to be a deviation in the first coefficient σ_1 of the grating varied line spacings from the specified values. Calculated values of the first VLS coefficient σ_1 are consistent with an estimate of the measurement uncertainty of the grating frequency for these coarse gratings.

From the different x-ray absorption spectra, an overall resolving power of about 3000 was measured, which is below the design goal of 5000. The source of this discrepancy could be the polishing errors of the M1 mirror and grating, the spatial resolution of the spectrometer detector, or vibrations of the optical elements. The quality of the zero order image shown in Figure 6 confirms that the figure errors of the optics and the spectrometer detector spatial resolution are sufficient to reach the energy resolution goal. At the time of the monochromator resolution characterization, vibrations observed in the motion of the zero order were significant. A 0.6 μrad error of the M1 mirror and grating angles may be assumed to include both polishing errors and vibrations. In this way, resolving powers about 3000 are calculated. During the commissioning time, improvements were made in the SXR monochromator. The support stands were grouted to the floor. Also, the original Ce:YAG crystal, 1 mm thick, was replaced by a crystal 220 μm thick, which could further improve the spatial resolution. In the future, it may be possible to reach the design resolution.

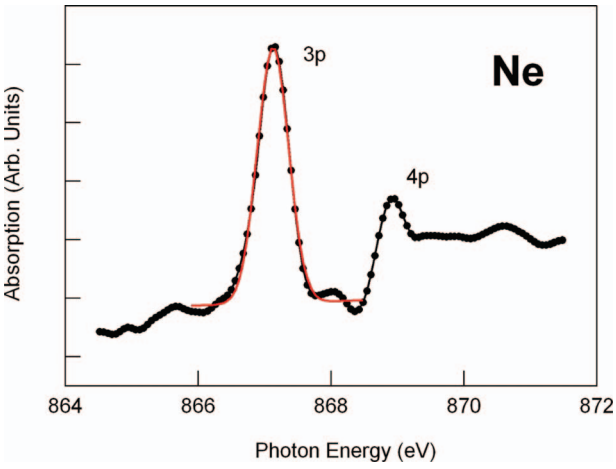

FIG. 8. (Color online) The neon 1*s* x-ray absorption spectrum taken with the 100 l/mm grating.

The photon energy calibration of the SXR monochromator was performed using different foils in the transmission sample chamber: Co, Ni, Cu, LaMnO, Tb, Gd, and Al. These samples were deposited through a mask onto Si_3N_4 windows such that only half of the window area was coated. By positioning the x-rays partly on the coated and partly on the uncoated Si_3N_4, the I_0 and I spectra are measured at the same time on different regions of the spectrometer detector image. In this way, a shot by shot normalization is possible.[17] The zero order was also measured with the beam on the unruled part of the grating and on the 100 and 200 l/mm rulings.

In summary, at the LCLS SXR instrument, the VLS grating monochromator provides a narrower bandwidth compared to the FEL source. A resolving power of 3000 has been achieved, which is within a factor of two of the design goal. Kirkpatrick-Baez mirrors produce a focus in the endstations with variable focus dimensions and focal distance.

ACKNOWLEDGMENTS

Portions of this research were carried out on the SXR instrument at the Linac Coherent Light Source (LCLS), a division of SLAC National Accelerator Laboratory and an Office of Science User Facility operated by Stanford University for the (U.S.) Department of Energy (DOE). The SXR instrument is funded by a consortium whose membership includes the LCLS, Stanford University through the Stanford Institute

for Materials Energy Sciences (SIMES), Lawrence Berkeley National Laboratory (LBNL), University of Hamburg through the BMBF priority program FSP 301, and the Center for Free Electron Laser Science (CFEL). This work was in part performed under the auspices of the DOE by Lawrence Livermore National Laboratory under Contract No. DE-AC52–07NA27344. Financial support for M.F.-P. was provided in part by Ministerio de Educacion y Ciencia, Programa Nacional de Movilidad de Recursos Humanos del Plan nacional de I+D+I 2008–2011. J.C., V.H., and L.J. acknowledge support from the Czech Ministry of Education within the Project No. ME10046 (KONTAKT).

[1]P. Emma, R. Akre, J. Arthur, R. Bionta, C. Bostedt, J. Bozek, A. Brachmann, P. Bucksbaum, R. Coffee, F. J. Decker, Y. Ding, D. Dowell, S. Edstrom, A. Fisher, J. Frisch, S. Gilevich, J. Hastings, G. Hays, P. Hering, Z. Huang, R. Iverson, H. Loos, M. Messerschmidt, A. Miahnahri, S. Moeller, H. D. Nuhn, G. Pile, D. Ratner, J. Rzepiela, D. Schultz, T. Smith, P. Stefan, H. Tompkins, J. Turner, J. Welch, W. White, J. Wu, G. Yocky, and J. Galayda, Nat. Photonics **4**(9), 641 (2010).

[2]J. Arthur, G. Materlik, R. Tatchyn, and H. Winick, Rev. Sci. Instrum. **66**(2), 1987 (1995).

[3]J. H. Underwood and J. A. Koch, Appl. Opt. **36**(21), 4913 (1997).

[4]J. Chalupsky, P. Bohacek, V. Hajkova, S. P. Hau-Riege, P. A. Heimann, L. Juha, J. Krzywinski, M. Messerschmidt, S. P. Moeller, B. Nagler, M. Rowen, W. F. Schlotter, M. L. Swiggers, and J. J. Turner, Nucl. Instrum. Methods Phys. Res. A **631**(1), 130 (2011).

[5]M. Martins, M. Wellhofer, J. T. Hoeft, W. Wurth, J. Feldhaus, and R. Follath, Rev. Sci. Instrum. **77**(11) (2006).

[6]R Soufli, M. J. Pivovaroff, S. L. Baker, J. C. Robinson, E. M. Gullikson, T. J. McCarville, P. M. Stefan, A. L. Aquila, J. Ayers, M. A. McKernan, and R. M. Bionta, Proc. SPIE **7077**, 707716 (2008).

[7]R. Soufli, M. Fernandez-Perea, S. L. Baker, J. C. Robinson, E. M. Gullikson, P. A. Heimann, W. F. Schlotter, and M. Rowen, "Development and calibration of mirrors and gratings for the Soft X-ray Materials Science beamline at the LCLS free-electron laser," Appl. Opt. (submitted).

[8]M. Sánchez del Río and R. J. Dejus, Proc. SPIE **3152**, 148 (1997).

[9]Joseph W. Goodman, *Introduction to Fourier Optics*, 2 ed. (McGraw-Hill, New York, 1996).

[10]See http://www.gsolver.com com for a description of the GSolver grating analysis program.

[11]See http://henke.lbl.gov/optical_constants for the index of refraction of elements and compound materials at x-ray photon energies.

[12]R. Soufli, A. L. Aquila, F. Salmassi, M. Fernandez-Perea, and E. M. Gullikson, Appl. Opt. **47**(25), 4633 (2008).

[13]R. A. London, R. M. Bionta, R. O. Tatchyn, and S. Roesler, Proc. SPIE **4500**, 51 (2001).

[14]S. P. Hau-Riege, R. A. London, A. Graf, S. L. Baker, R. Soufli, R. Sobierajski, T. Burian, J. Chalupsky, L. Juha, J. Gaudin, J. Krzywinski, S. Moeller, M. Messerschmidt, J. Bozek, and C. Bostedt, Opt. Express **18**(23), 23933 (2010).

[15]H. Petersen, C. Jung, C. Hellwig, W. B. Peatman, and W. Gudat, Rev. Sci. Instrum. **66**, 1 (1995).

[16]M. Kato, Y. Morishita, M. Oura, and H. Yamaoka, J. Electron Spectrosc. Relat. Phenom. **160**, 39 (2007).

[17]D. P. Bernstein, Y. Acremann, A. Scherz, M. Burkhardt, J. Stohr, M. Beye, W. F. Schlotter, T. Beeck, F. Sorgenfrei, A. Pietzsch, W. Wurth, and A. Fohlisch, Appl. Phys. Lett. **95**(13) (2009).